A Symmetric Time-Varying Cluster Rate of Descent Model

Eric S. Ray[1]

MRI Technologies, Houston, TX, 77058

A model of the time-varying rate of descent of the Orion vehicle was developed based on the observed correlation between canopy projected area and drag coefficient. This initial version of the model assumes cluster symmetry and only varies the vertical component of velocity. The cluster fly-out angle is modeled as a series of sine waves based on flight test data. The projected area of each canopy is synchronized with the primary fly-out angle mode. The sudden loss of projected area during canopy collisions is modeled at minimum fly-out angles, leading to brief increases in rate of descent. The cluster geometry is converted to drag coefficient using empirically derived constants. A more complete model is under development, which computes the aerodynamic response of each canopy to its local incidence angle.

Nomenclature

A	=	Amplitude of fly-out angle or projected area sinusoidal waveform
A_0	=	Amplitude shift of fly-out angle or projected area sinusoidal waveform
C_{D_o}	=	Drag coefficient related to full open canopy, normalized to total system weight and rate of descent
$(C_DS)_V$	=	Effective drag area of test vehicle
CDT	=	Cluster Development Test (series)
CPAS	=	Capsule Parachute Assembly System
Δt	=	Fly-out angle or projected area sinusoidal phasing term
Δt_{sync}	=	Sinusoidal phasing term for synchronization of damped epoch
Δt_{trans}	=	Time to transition from transient epoch to damped epoch
D_o	=	Nominal parachute diameter based on constructed area, $D_o = \sqrt{4 \cdot S_o / \pi}$
D_p	=	Projected diameter of a parachute, $D_p = \sqrt{4 \cdot S_p / \pi}$
EDU	=	Engineering Development Unit
GPS	=	Global Positioning System
HD	=	High Definition (camera)
K	=	Projected area amplitude reduction factor to emulate canopy collisions
L_R	=	Reefing line length
L_s	=	Suspension line length
MPCV	=	Multi Purpose Crew Vehicle (Orion)
N_c	=	Number of parachutes in a cluster
N_w	=	Number of waveforms in fly-out angle sinusoidal construction
$\bar{q}$, qbar	=	Dynamic pressure
ρ	=	Humidity-corrected atmospheric density
RC	=	Ramp Clear (usually chosen as start of test)
SD	=	Standard Definition (camera)
S/N	=	Serial Number
S_o	=	Parachute Canopy open reference area based on constructed shape
S_p	=	Projected frontal canopy area
S_{P_c}	=	Projected frontal canopy area of a cluster
t	=	Elapsed time
T	=	Period of fly-out angle or projected area sinusoidal waveform

---

[1] Analysis Engineer, Aeroscience and Flight Dynamics, 2224 Bay Area Blvd, Houston, TX, AIAA Member.

American Institute of Aeronautics and Astronautics

$T_{1/2}$	=	Projected area half-cycle counter to emulate parachute collisions
θ_i, theta	=	Fly-out angle for parachute i
θ_b	=	Bias in fly-out angle waveform
t_{trans}	=	Relative time from inflation to start of transition from transient epoch to damped epoch
V_e	=	Equilibrium rate of descent
W_T	=	Total weight of test vehicle and parachutes

I. Introduction

THE Capsule Parachute Assembly System (CPAS) is designed to safely decelerate the Orion Multi Purpose Crew Vehicle (MPCV) to an ocean splashdown.[1] The final sequence in the system are the 116 ft D_o ringsail Main parachutes. The sequence nominally deploys a cluster of three Mains, but the system must meet landing requirements with only two deployed Mains.

The Main canopy design was modified with added geometric porosity during the second generation of testing in order to reduce cluster dynamics.[2] The resulting Engineering Development Unit (EDU) design is shown in Fig. 1. A gap was created on sail 2 by removing material around the circumference, and a panel was removed from every fifth panel of sail 7.
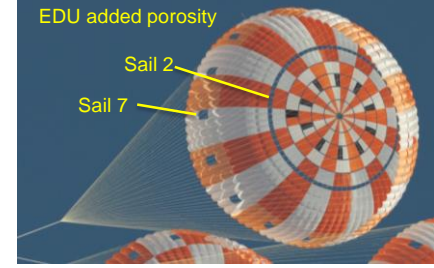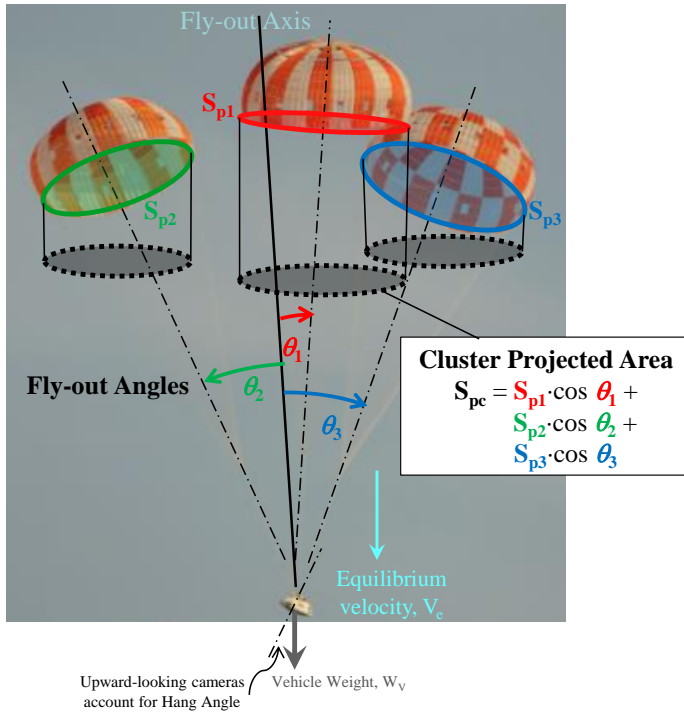

Figure 1. EDU Main design with added porosity.

An understanding of the instantaneous performance of the Main parachute cluster is necessary to properly simulate the MPCV velocity and orientation at splashdown. The CPAS test program closely measured the steady-state rate of descent with onboard Global Positioning System (GPS) instrumentation[3] as well as the cluster geometry through photogrammetrics[4]. Canopy positions are measured by the "fly-out angle" (θ) between each canopy centerline and a central axis. A direct relationship between the cluster projected area (illustrated in Fig. 2) and the instantaneous vertical drag coefficient (C_{Do} defined in Eq. (1)) was previously established in Ref. 5. This relationship provides a convenient way to model cluster temporal performance.

Figure 2. Main cluster steady-state geometry.

$$C_{D_o} = \frac{1}{N_c \cdot S_o} \cdot \left(\frac{W_T}{\frac{1}{2} \cdot \rho \cdot V_e^2} - (C_D S)_V \right) \qquad (1)$$

When the canopies fly-out to their maximum extent, the induced torque is highest, the drag coefficient is slightly lowered, and therefore the rate of descent increases slightly. Yet when the canopies come to their minimum fly-out and "collide" with each other, a significant amount of cluster projected area (S_{pc}) is lost, the drag coefficient is

2

American Institute of Aeronautics and Astronautics

significantly lowered, and the system will quickly accelerate to a higher rate of descent. To demonstrate this effect, the individual canopy and total cluster projected areas for Cluster Development Test (CDT)-3-3 are plotted on the primary y-axis in Fig. 3. The drag coefficient (light blue) is plotted on the secondary y-axis. These parameters can be directly related by adjusting the scale factor (SF) between axes. The vertical grey bars indicate observed collisions between canopies, where the sudden loss in cluster projected areas and drag coefficient are most evident. A slight lag is noticeable from when the cluster behavior is observed by the cameras and when the behavior manifests in the drag, as measured by a GPS at the vehicle.
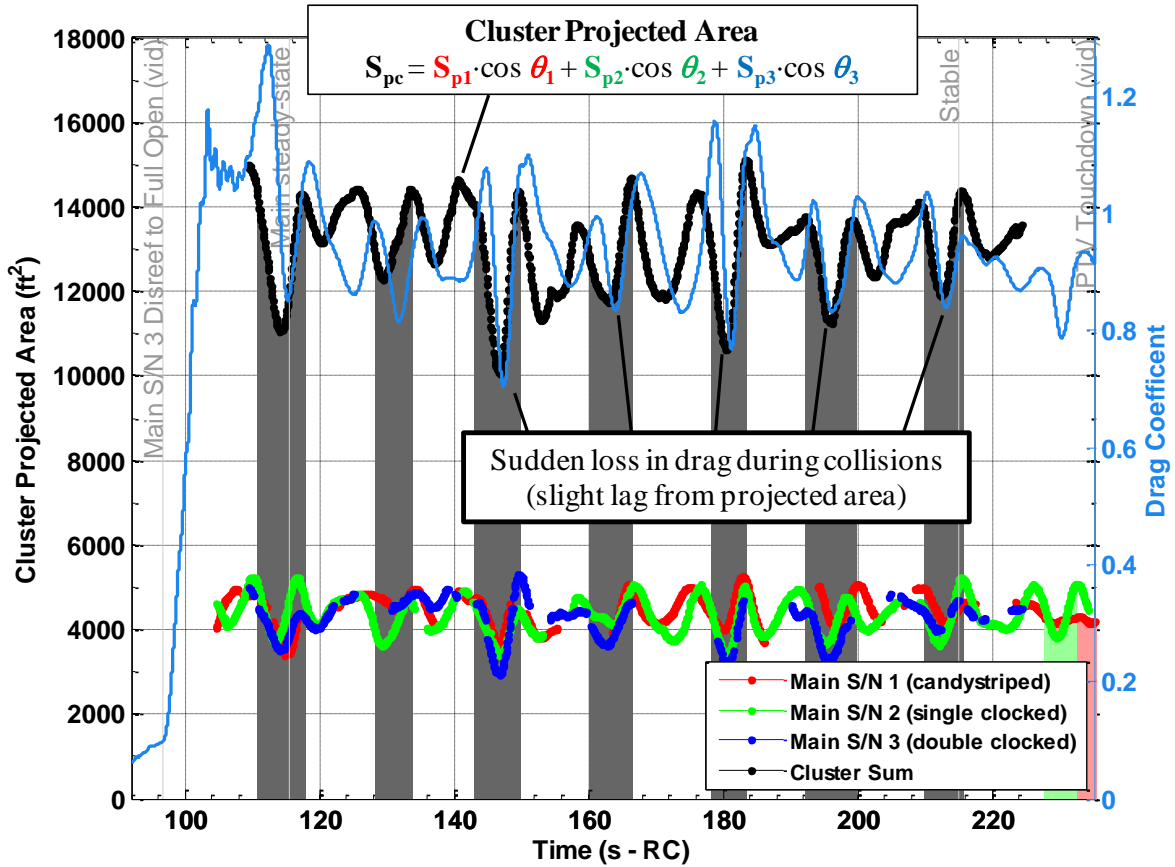

Cluster Projected Area
$$S_{pc} = S_{p1} \cdot \cos \theta_1 + S_{p2} \cdot \cos \theta_2 + S_{p3} \cdot \cos \theta_3$$

Sudden loss in drag during collisions
(slight lag from projected area)

Main S/N 1 (candystriped)
Main S/N 2 (single clocked)
Main S/N 3 (double clocked)
Cluster Sum

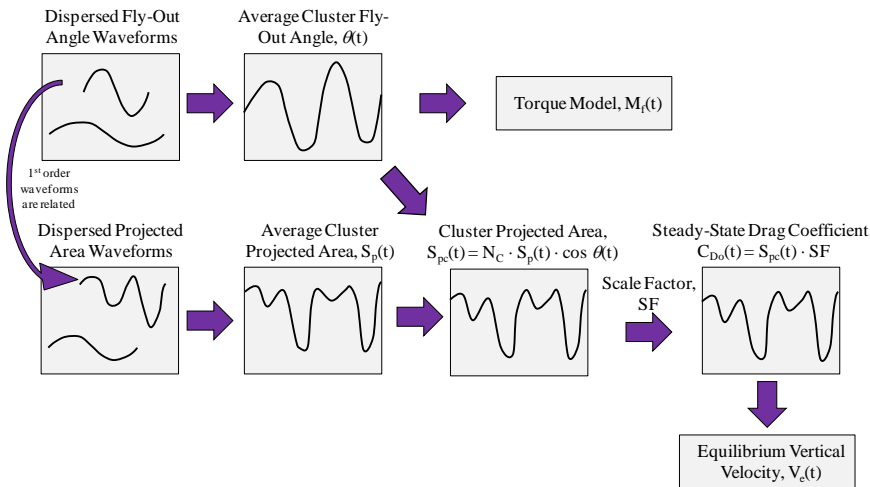**Figure 3. Correlation between Main cluster projected area and drag coefficient.**

Figure 4. Time-varying simulation flow diagram.

This observed relationship between cluster geometry and vertical performance is the source of the time-varying rate of descent model, as shown in the flow diagram in Fig. 4. First, the variations of parachute geometry are modeled with a series of sine waves, whose parameters are derived from flight test video photogrammetric measurements. The modeled fly-out angles and projected areas are then propagated into models of torque model and drag coefficient. Finally, the drag coefficient variation will drive the variation in the equilibrium velocity. Besides the nominal time-varying nature of the simulation,

3

American Institute of Aeronautics and Astronautics

parameters are dispersed based on test-to-test variation, resulting in different results from Monte Carlo simulations. At each step, models are compared with test data to ensure results are in family with test experience.

For simplicity, the geometric models assume radial symmetry. The fly-out angles and projected areas are assumed equal between canopies, so average values are used. Further, the model is based on analysis of purely vertical velocity, where no additional incidence angle is computed based on the position of canopies relative to wind fields. A model where individual canopies are modeled according to local aerodynamic incidence angles is currently under development.

The various models for steady-state descent are each described in sub-sections within this section. The parameters used for the fly-out model and projected area are separated into two-Main and three-Main cases. Furthermore, these models are divided into phases (or epochs), based on the observed state changes in cluster stability characteristics. Typical behavior during both epochs is listed in Table 1. Each simulation run should internally compute variables using both sets of parameters and then transition from one to the other over a specified time for the final "blended" output.

Table 1. EDU Main Time-Varying C_D Model Parameters

	Early Phase: Transient Epoch	More Stable Phase: Damped Epoch
Rate of Descent, V_{eo}	Large variation	Higher average, but less variation
Fly-Out Angles, θ	Most extreme values immediately after inflation	Lower amplitude but similar average as transient
Projected Area, S_p	Most drag produced per unit projected area	Least drag produced per unit projected area
Canopy Collisions	Regularly strong	Infrequent or glancing

II. Fly-Out Angles

Whenever possible, fly-out angle parameters were determined through reconstruction of all relevant EDU test data. Reconstructions of CDT-2-2 and CDT-2-3 data have also been applied. These tests had the same added geometric porosity as the EDU tests, but had not yet incorporated the longer Main line length ratio of 1.4.

A. Fly-Out Angle Frequency Analysis

Fly-out angle data is provided as equally time spaced angular values (in degrees from the computed centroid) at a 5 or 10 samples per second rate. This data stream provides a classic time series that may be analyzed using statistical methods.

Time series analysis allows the data stream to be broken into three components: linear trend (slope and intercept), periodic signal, and residual, random errors. The linear effects can be removed using standard linear regression techniques. The linear terms are then subtracted from the time series. This leaves de-trended data with an approximate mean and slope of 0. These elements can then be re-combined with some variation to create a realistic time-varying fly-out model, as illustrated in Fig. 5.
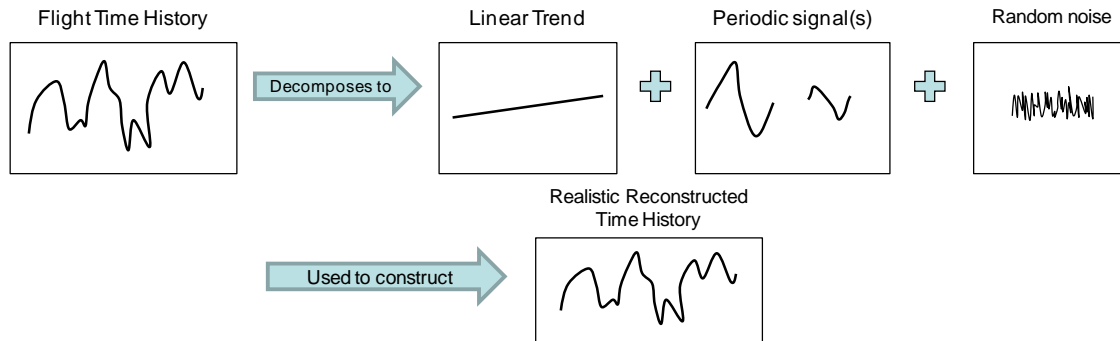

Figure 5. Fly-out data reduction overview.

Autocorrelation techniques are applied to the de-trended data to identify positively correlated periods from the time stream. Autocorrelation determines the correlation of one observation with another at a fixed number of observations away (lag). This analysis is conducted on all of the observations. Based on the number of observations processed, the statistical significance of the autocorrelation values can be determined. A program called "Deperiod.exe." has been developed to conduct the autocorrelation processing of the time series and offers manual or automated selection of the periods.

The automated selection process identifies the significant positive correlation peaks. The program looks for the most significant peak. If the peak selected is the initial (lowest period) peak, then harmonic peaks are evaluated, if present, and are used to refine the peak period. Once the period has been selected, the data stream is processed to normalize observations based on the centered moving average of the period length. Each adjusted observation is then averaged with the other observations spaced one period length apart. This results in a period long set of data defining the waveform, including phase and shape. The waveform is then subtracted from the observations using the modulus function ("MOD") so that the same waveform is sequentially removed from the observations. The remaining data is considered the residuals.
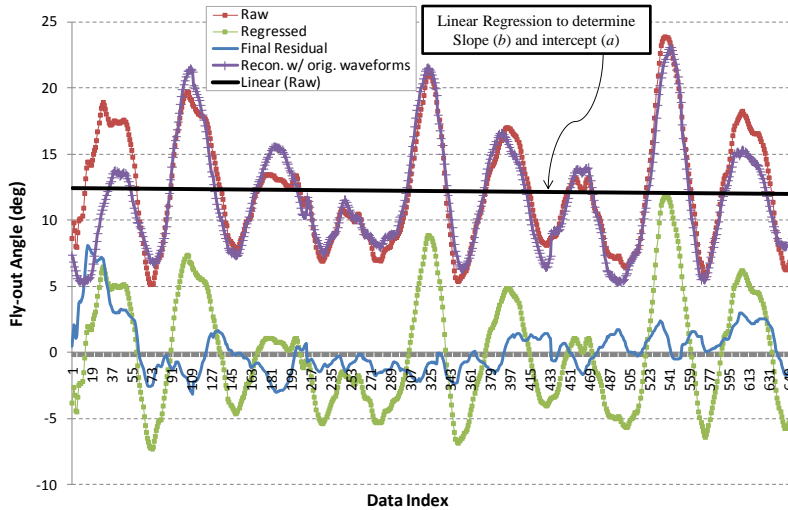
The residuals are then reprocessed starting with the removal of any remaining linear effects, and then analyzed for periodic effects. The program is currently set to do this up to three times. This results in a linear model (slope and intercept) and up to three waveforms. The data stream can be reconstructed from these terms by summation of the linear and periodic terms (both waveform and phase).

The impact of each step of the process is evaluated in terms of the reduction of the data variance. An example reduction of a fly-out time history for an example two-Main flight test is shown in Fig. 6. Three periodic signals were removed from the data resulting in a small residual. The original wave forms were then re-applied to demonstrate a good match with the original data.

Figure 6. Sample fly-out angle regression of typical two-Main test.

The first order periodic signal from the sample two-Main test is shown in Fig. 7. It can be seen that the waveform appears sinusoidal. Therefore, the proposed fly-out angle model uses sine waves for computational simplicity.
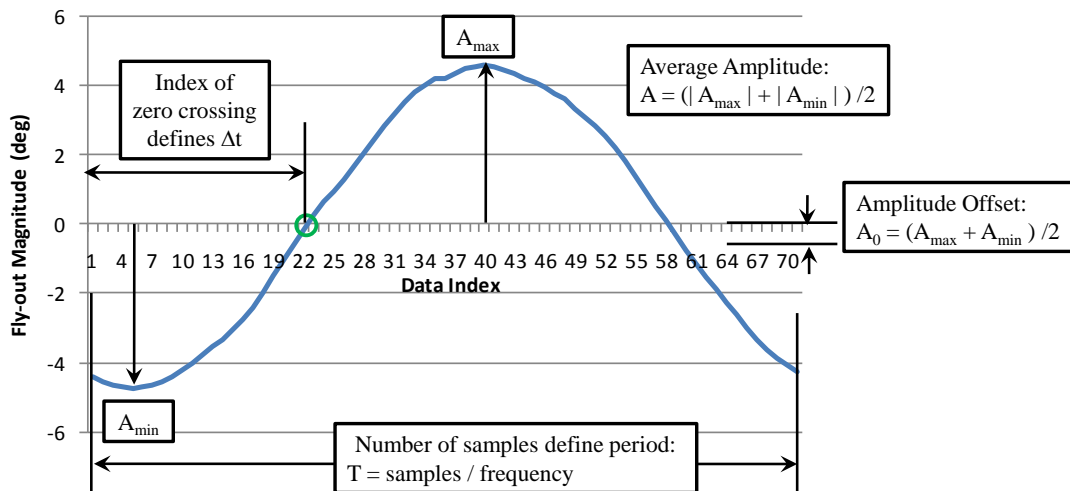

Figure 7. First order waveform from sample two-Main test.

5

American Institute of Aeronautics and Astronautics

B. Fly-Out Angle Model

The fly-out angle model consists of the summation of a constant bias and up to three sine waves of different magnitude, frequency, time shift, and amplitude shift. Each parachute in the cluster is assumed to have the same fly-out, so only one calculation needs to be made for the cluster for each epoch. Separate fly-out computations should be made for the transient epoch and damped epoch and then "blended" together during a transition period.

In order to implement this model in a Monte Carlo simulation for a specific parachute configuration, the model parameters are randomly selected based on pre-generated dispersions tables. The generic fly-out angle, θ, as a function of time is determined by Eq. (2):

$$\theta(t) = \theta_b + \sum_{i=1}^{N_w} \theta_i(t) \tag{2}$$

Where:

t	[sec]	Time from model initiation
θ_b	[deg]	Waveform bias angle
N_w	[ND]	Total number of sine waves
$\theta_i(t)$	[deg]	i^{th} order sine wave $\qquad = A \cdot \sin\left(\dfrac{2 \cdot \pi \cdot (t - \Delta t)}{T}\right) + A_0$
A	[deg]	Sine wave peak amplitude
Δt	[sec]	Sine wave time shift
T	[sec]	Sine wave period
A_0	[deg]	Sine wave amplitude shift

An example of a fly-out angle reconstruction is shown in Fig. 8 for a typical three-Main test. The goal was to match the average fly-out angle (black) for both the transient epoch and damped epoch. Data from each of the circled regions was input into the Deperiod.exe to determine waveform parameters and some adjustments were made manually to generate the modeled traces (purple). The model will transition from the transient epoch after a relative time of t_{trans} and complete the transition to the damped epoch over a duration of Δt_{trans}.

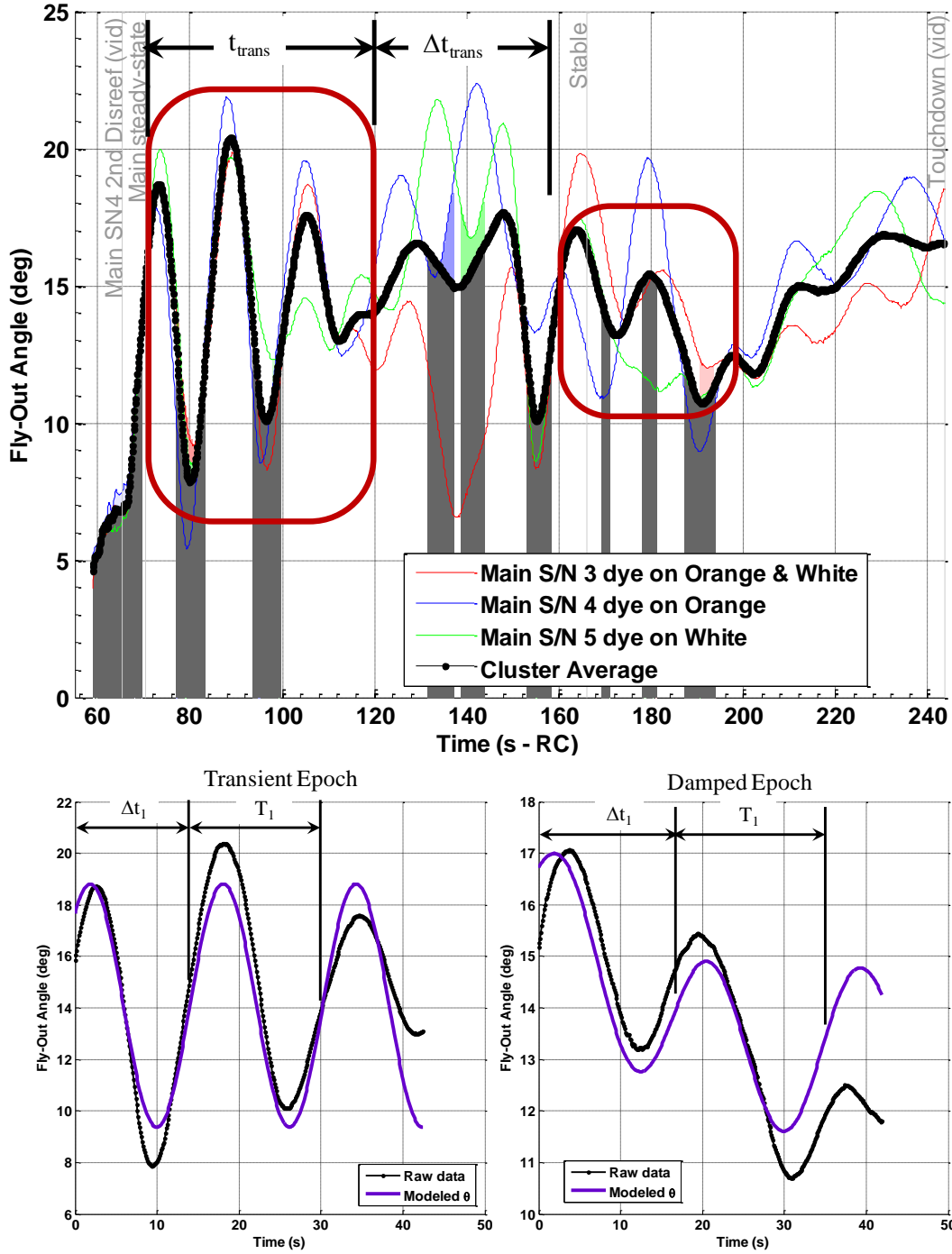American Institute of Aeronautics and Astronautics

Figure 8. Typical three-Main fly-out angle reconstruction of transient epoch and damped epoch.

An additional change must be made to the phasing of the damped epoch fly-out angle model in order to synchronize with the test data. The damped data were reduced starting at $t_{trans} + \Delta t_{trans}$ after the start of steady-state. If the damped model is started at the beginning of steady-state, the resulting trace (cyan) will not coincide with the test data, as seen in Fig. 9. A synchronized phasing term for each damped epoch waveform (Δ_{tsync}) should be computed based on how many periods occur during the transition according Eq. (3). These new phasing terms should be used to generate the damped epoch model. However, the original fly-out phasing term (Δt_1) should be retained in order to later generate the first order projected area waveform (Section II B).

7

American Institute of Aeronautics and Astronautics

$$1^{st} \text{ Order:} \quad \Delta t_{sync1} = mod(t_{trans} + \Delta t_{trans} + \Delta t_1, T_1)$$
$$2^{nd} \text{ Order:} \quad \Delta t_{sync2} = mod(t_{trans} + \Delta t_{trans} + \Delta t_2, T_2) \qquad\qquad\qquad (3)$$
$$3^{rd} \text{ Order:} \quad \Delta t_{sync3} = mod(t_{trans} + \Delta t_{trans} + \Delta t_3, T_3) \qquad (if\ present)$$

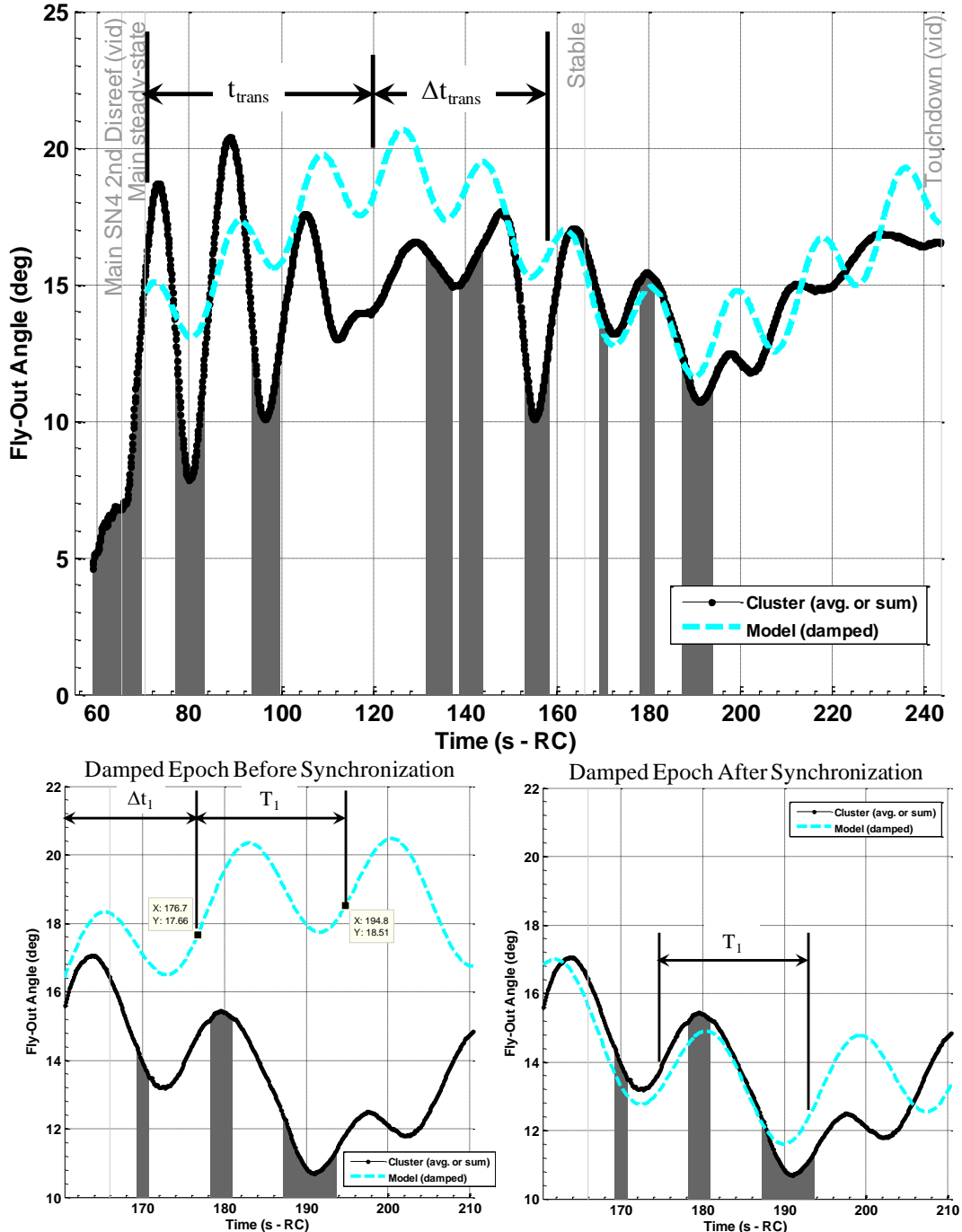The damped model with the adjusted phasing is shown to match the test data after the transition in Fig. 9.

Figure 9. Adjusted fly-out angle phasing for damped epoch (top); close-up of damped epoch before (lower left) and after (lower right) phasing adjustment.

American Institute of Aeronautics and Astronautics

The transient fly-out model (magenta) is then "blended" with the damped fly-out model (cyan) over the duration of Δt_{trans}, as shown in Fig. 10. This linear blending with time results in the final fly-out model (purple) which generally matches the original test data (black).
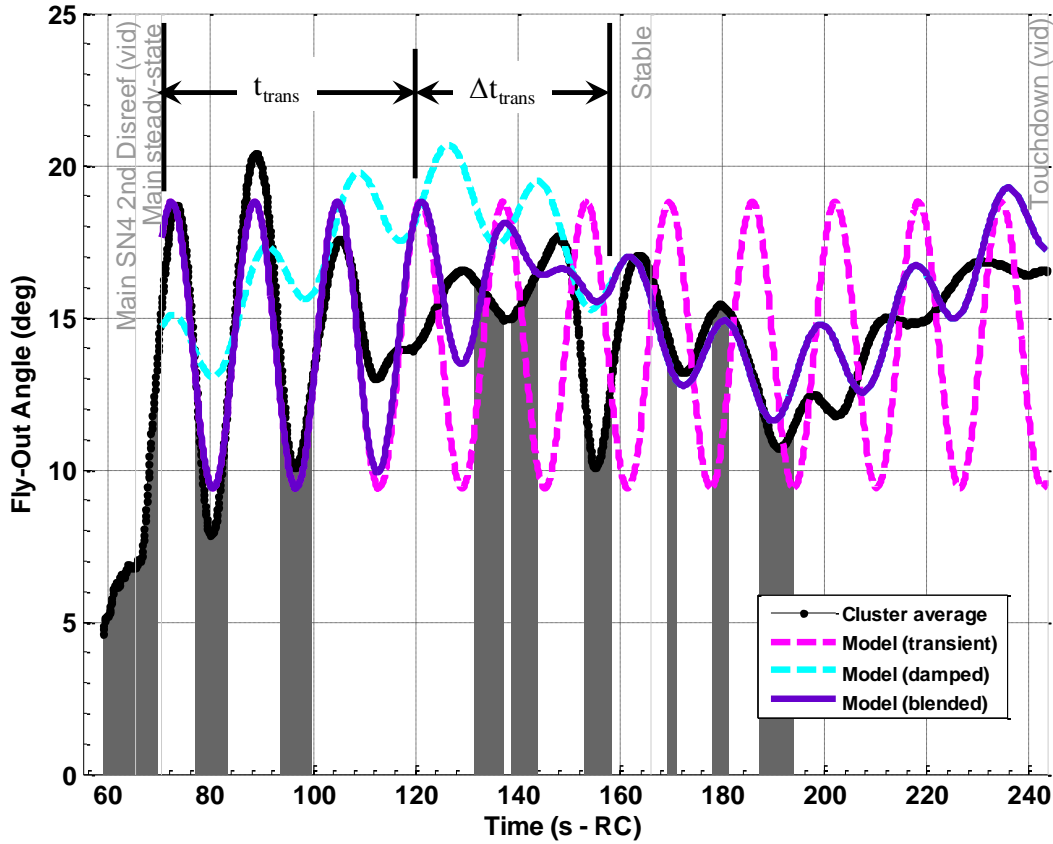

Figure 10.   Fly-out transient epoch model (magenta) and damped epoch model (cyan) are linearly blended (purple) with time over a duration of Δt_{trans}.

III. Projected Area

The projected area model is similar to the fly-out angle model in that it uses sinusoidal waveforms to simulate observed test oscillations. However, the primary waveform is modified to account for the sudden loss in projected area when the parachutes collide at the minimum fly-out angle.

A. Projected Area Measurements

Like the fly-out angles, projected area measurements are derived from tracking points on upward-looking video, as seen on the left of Fig. 11, and as described in Ref. 5. The procedure is more intensive than that for fly-out dynamics, because ten points are tracked along the skirt of each canopy, rather than the single point at each vent. This also means that data are lost when enough of a canopy moves out of frame, while the vents are more likely to stay within frame. The 2-D tracked points are converted to 3-D by estimating the distance to the camera. All skirt points are assumed to lie on the surface of a sphere centered at the camera, as seen on the right of Fig. 11. The radius of this theoretical sphere is based on the riser length, suspension line length, and a typical skirt diameter. The projected area is computed as the sum of circular sectors. It can be seen from the two frames on the left that the area is greatly reduced when canopies come into contact. The data show that projected area is also slightly reduced when the canopies are furthest apart due to canopy deformation.
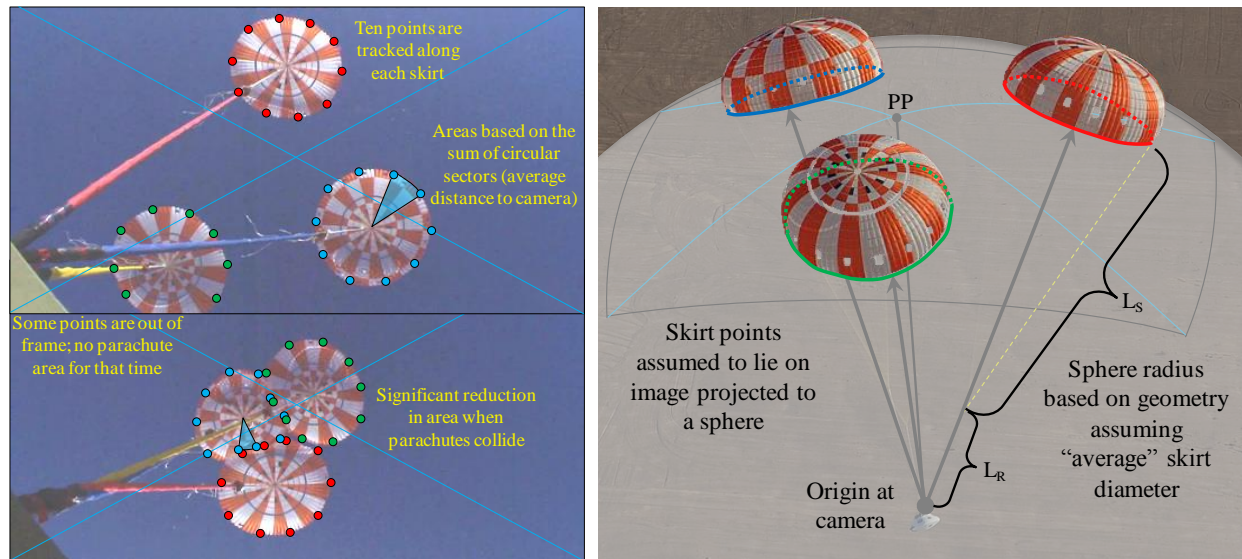
American Institute of Aeronautics and Astronautics

Figure 11.   Canopy projected area measurements.

B. Projected Area Model

While the Deperiod.exe code is successful in decomposing the fly-out angle waveforms, it has not been successful in deconstructing the more complicated projected area waveforms. Therefore, all analysis has been performed manually.

The first order mode ($i = 1$) of projected area was derived from observed correlation with fly-out angles. As illustrated in Fig. 12, when fly-out angles are at their maximum, there is a small reduction in average projected area but the largest negative amplitude occurs during a canopy collision. A second order mode ($i = 2$) will account for the variation in minima from collision to collision.
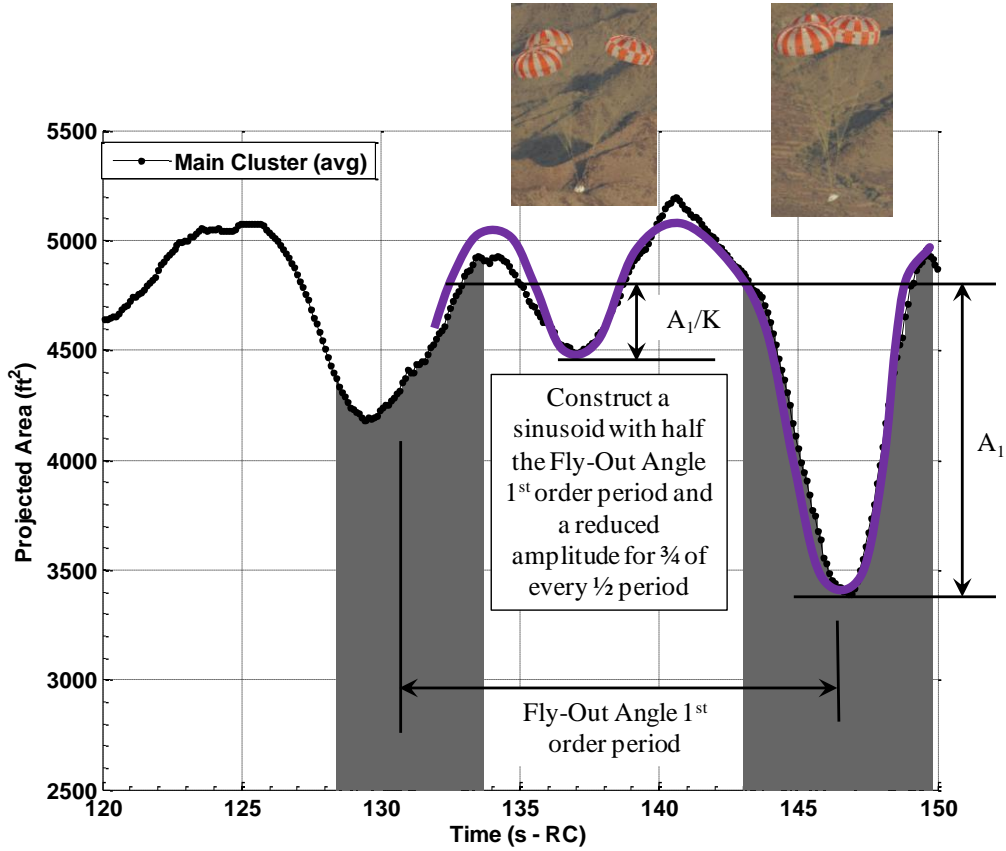
American Institute of Aeronautics and Astronautics

Figure 12.   Primary projected area mode.

The projected area is a sum of waveforms which are each produced by the general form of Eq. (4). Parameters A_1 and K are determined from test data by averaging the maximum points as well as the major and minor minimum points.

$$S_{p_i}(t) = A \cdot \sin\left(\frac{2 \cdot \pi \cdot (t - \Delta t)}{T}\right) + A_0 \tag{4}$$

A reconstructed first order fly-out angle waveform is plotted in pink in Fig. 13. In order to capture the desired canopy collision features, the first order projected area waveform must have a wavelength half as long as the fly-out angle wavelength (or twice the frequency). That waveform is plotted as a dotted curve in the upper plot. In order for the projected area minimum to coincide with a fly-out angle minimum, the projected area wave is shifted to the left by 1/8 of a fly-out angle period (dashed curve). Therefore, the first order projected area phasing (Δt_1) is entirely dependent on the fly-out angle phasing and period. In the lower plot, the first order amplitude (A_1) is reduced by a factor of K for ¾ of its double cycle. The final first order waveform, plotted as a solid purple trace, matches the desired shape. The projected area timing terms are summarized in Eq. (5), which should be applied to both the transient and damped epoch terms (additional damped epoch synchronization is applied later).
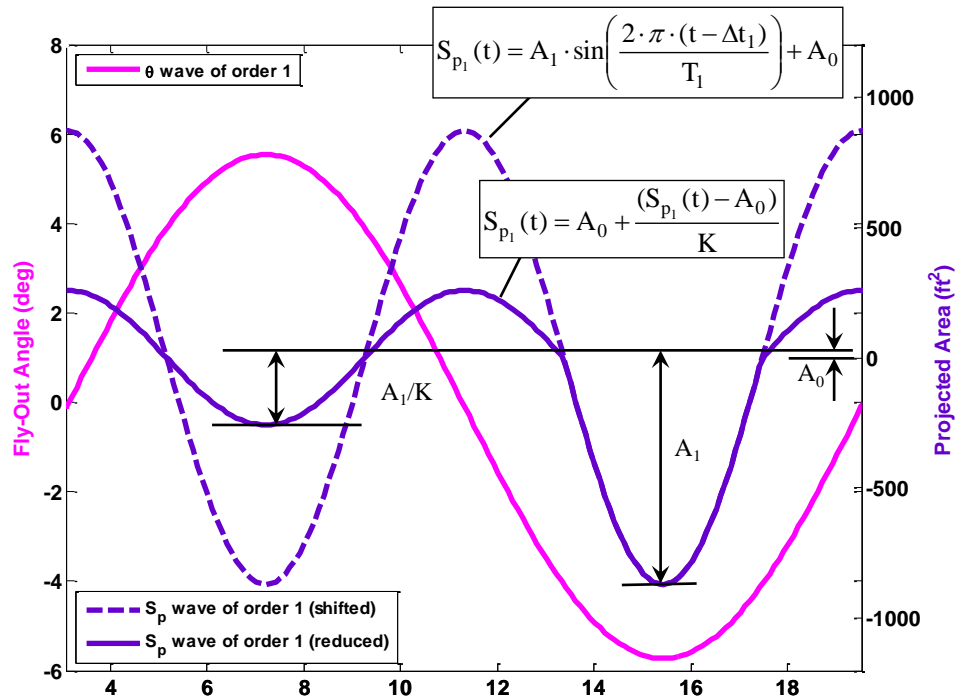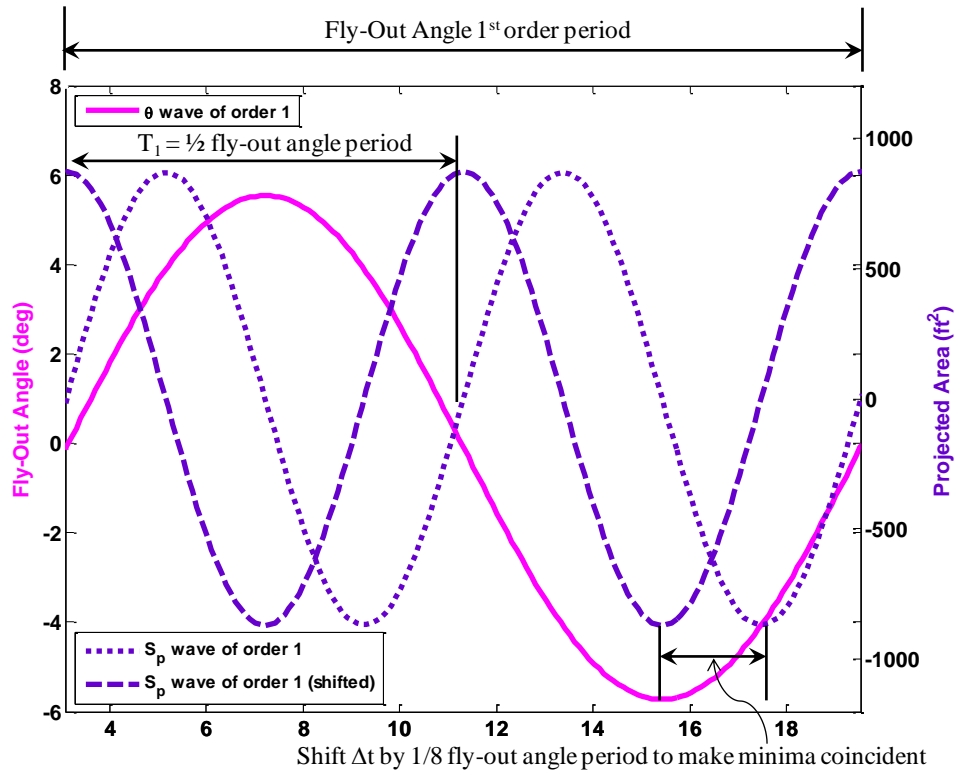
American Institute of Aeronautics and Astronautics

Fly-Out Angle 1st order period

$$S_{p_1}(t) = A_1 \cdot \sin\left(\frac{2 \cdot \pi \cdot (t - \Delta t_1)}{T_1}\right) + A_0$$

$$S_{p_1}(t) = A_0 + \frac{(S_{p_1}(t) - A_0)}{K}$$

Figure 13. **Construction of primary projected area mode from primary fly-out angle mode.**

American Institute of Aeronautics and Astronautics

$$(T_1)_{area} = \frac{(T_1)_{fly-out}}{2}$$

$$(\Delta t_1)_{area} = (\Delta t_1)_{fly-out} - \frac{(T_1)_{fly-out}}{8} \tag{5}$$

The times at which to reduce the amplitude are defined by counting the number of half-cycles ($T_{1/2}$) using the modulo operator ("mod" internal MATLAB function), as in Eq. (6).

$$T_{1/2} = \text{mod}((t - \Delta t_1)/(T_1/2), 4) \tag{6}$$

For example, the $T_{1/2}$ counter is plotted vs. time in Fig. 14. The amplitude should be reduced by the scale factor whenever the counter is 3 or below, as summarized in Eq. (7).
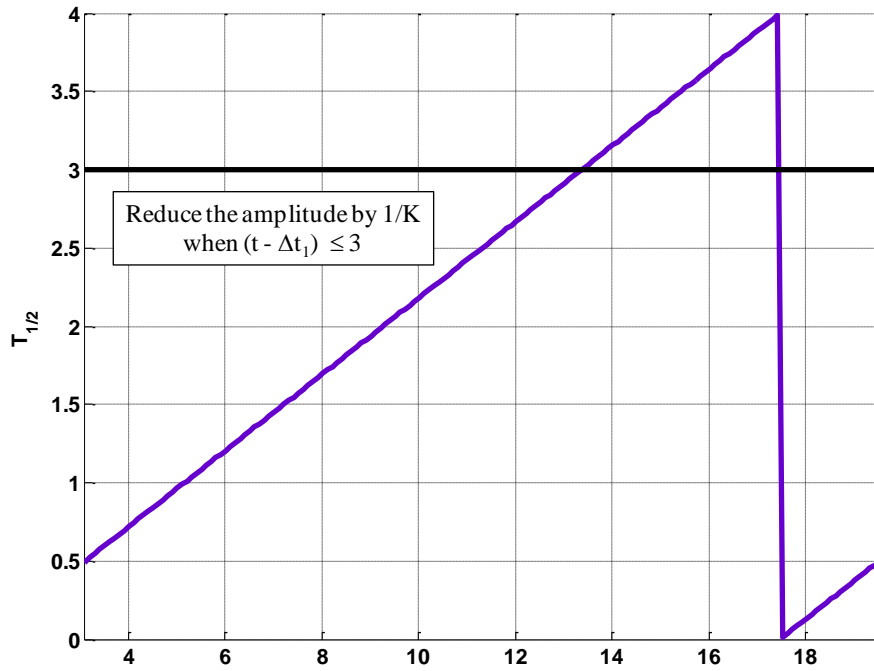
Figure 14.   Counting the number of half-cycles in the primary mode.

$$S_{p_1} = \begin{cases} A_0 + \dfrac{(S_{p_1} - A_0)}{K} & \text{if } T_{1/2} \leq 3 \\[2em] S_{p_1} & \text{if } T_{1/2} > 3 \end{cases} \tag{7}$$

A second order mode completes the projected area model by varying the severity of the canopy collisions with time. The second order waveform parameters were determined empirically for each available test by manually constructing a sine wave to intersect with as many minimum points as possible. This process emphasized matching the low drag/high rate of descent features, leading to a conservative model (e.g. simulating higher impact velocities).

Once the individual waveforms are established, the average projected area, S_p, is computed as a function of time with Eq. (8), which is analogous to fly-out angle Eq. (2) (except there are always only two waveforms for projected area). The bias term (S_{p_b}) is dispersed based on multiple flight test reconstructions.

$$S_p(t) = S_{p_b} + S_{p_1}(t) + S_{p_2}(t) \tag{8}$$

13

American Institute of Aeronautics and Astronautics

During the damped epoch, the projected area model requires some phasing adjustment similar to the fly-out angle model. However, because the first order projected area period is half that of the first order fly-out angle period, the adjustment to the projected area phasing requires a shifting based on twice the projected area period, as in Eq. (9). This ensures that the fly-out angle minima are synchronized with the projected area minima during the damped epoch, as in Fig. 15.

$$1^{st} \text{ Order:} \qquad \Delta t_{sync1} = \text{mod}(t_{trans} + \Delta t_{trans} + \Delta t_1, \mathbf{2 \cdot T_1})$$
$$2^{nd} \text{ Order:} \qquad \Delta t_{sync2} = \text{mod}(t_{trans} + \Delta t_{trans} + \Delta t_2, T_2) \qquad (9)$$
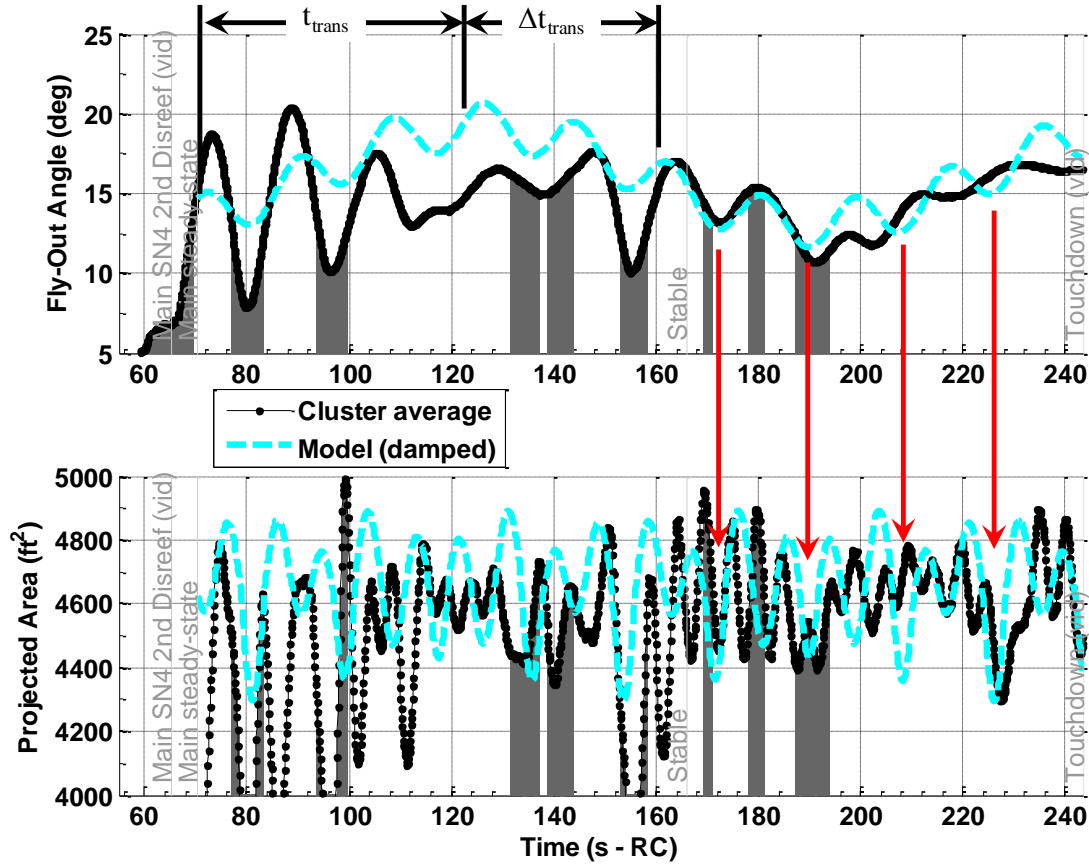

Figure 15. **Synchronization of projected area damped epoch model with fly-out angle model.**

The blending of the projected area from the transient epoch model to the damped epoch is performed over the same time period as that of the fly-out angle. The final model (purple) matches the test data (black) as in Fig 16.
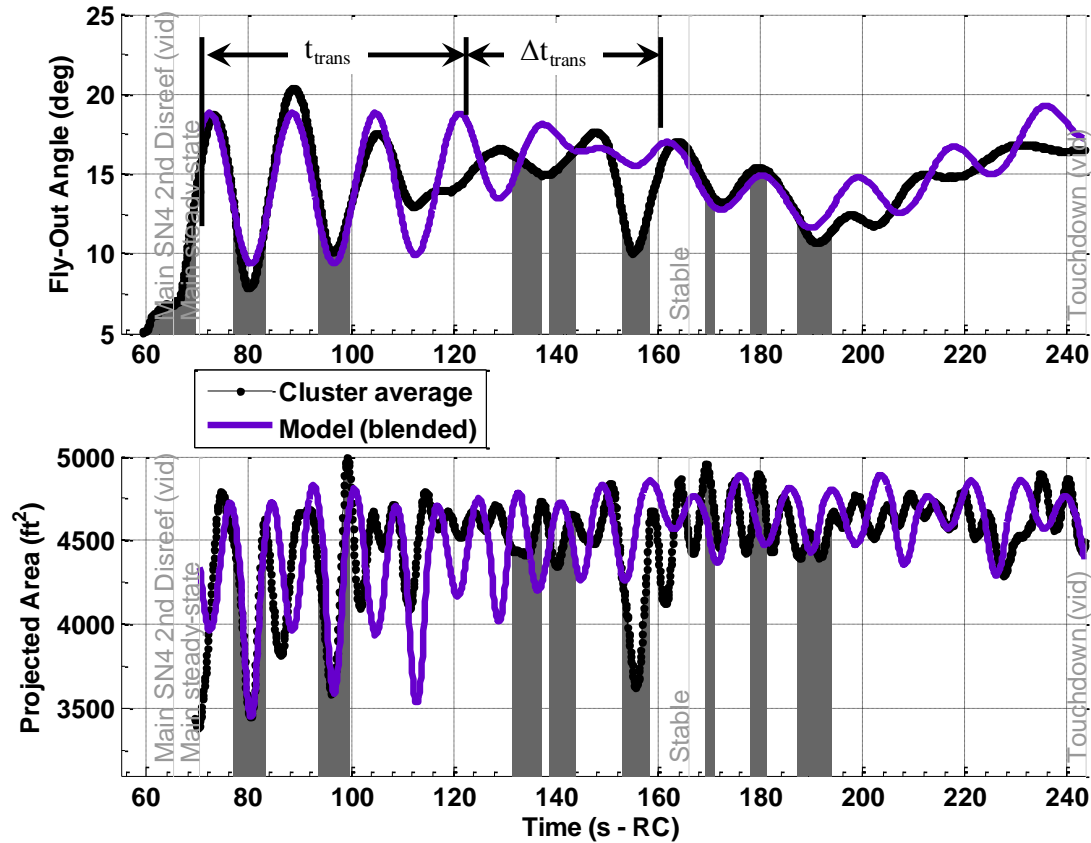
American Institute of Aeronautics and Astronautics

Figure 16.   Blended fly-out angle and projected area models compared with flight data.

Reconstructions of all available flight tests were used to generate nominal and dispersed projected area parameters. These parameters are collected for two-Main and three-Main cases in the Model Memo.

IV.   Drag Coefficient and Rate of Descent

As mentioned earlier, examination of flight tests show that the cluster projected area is directly proportional to the vertical drag coefficient, C_{Do}. A scale factor, SF, is defined for both the transient epoch and damped epoch as the average drag coefficient divided by the average cluster projected area for each particular region. The scale factor during the transient epoch is defined such that the minima are captured, as illustrated in Fig. 17. The scale factor during the damped epoch, shown in Fig. 18, is relevant for more stable cluster dynamics. These empirically-derived scale factors are specific to the particular planform design and would have to be re-derived for different canopies.
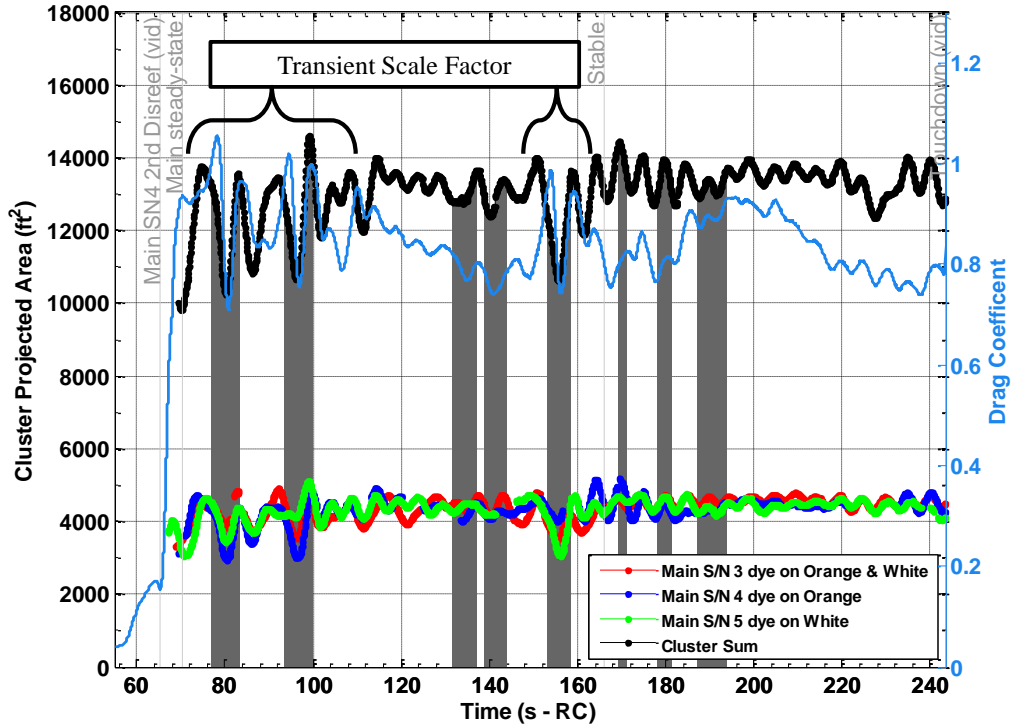
American Institute of Aeronautics and Astronautics

Figure 17.   Scale factor between cluster projected area and drag coefficient for three-Main transient epoch.
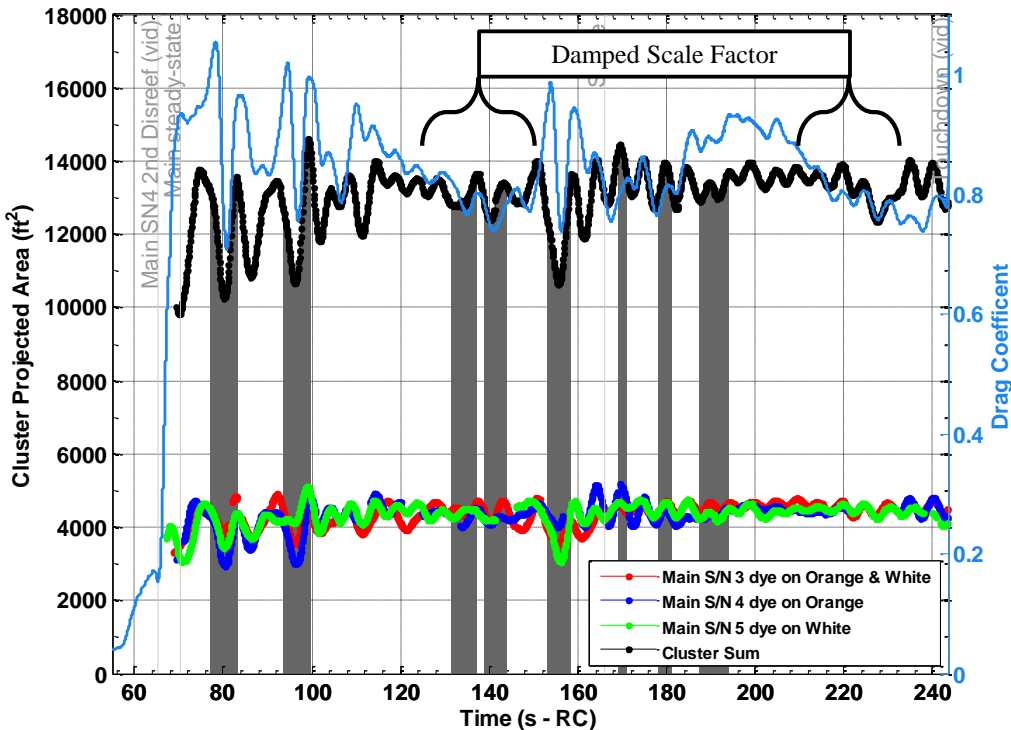

Figure 18.   Scale factor between cluster projected area and drag coefficient for three-Main damped epoch.

The drag coefficient scale factor can therefore be blended during the transition from the transient to damped epoch along with fly-out angle and projected area models. A blending factor, f_{blend}, varies linearly with time during the transition period as in the following pseudo-code:

American Institute of Aeronautics and Astronautics

```
if (t < t_trans)
    % time before start of blending
    θ(t) = (θ)_transient
    S_p(t) = (S_p)_transient
    SF(t) = (SF)_transient
elseif (t < t_trans + Δt_trans)
    % fraction of time within blending period
    f_blend = (t - t_trans)/Δt_trans
    θ(t) = (θ)_transient * (1- f_blend) + (θ)_damped * f_blend
    S_p(t) = (S_p)_transient * (1- f_blend) + (S_p)_damped * f_blend
    SF(t) = (SF)_transient * (1- f_blend) + (SF)_damped * f_blend
else
    % time past blending
    θ(t) = (θ)_damped
    S_p(t) = (S_p)_damped
    SF(t) = (SF)_damped
end
```

The transition for each of these states for the example three-Main test reconstruction is shown in Fig. 19.

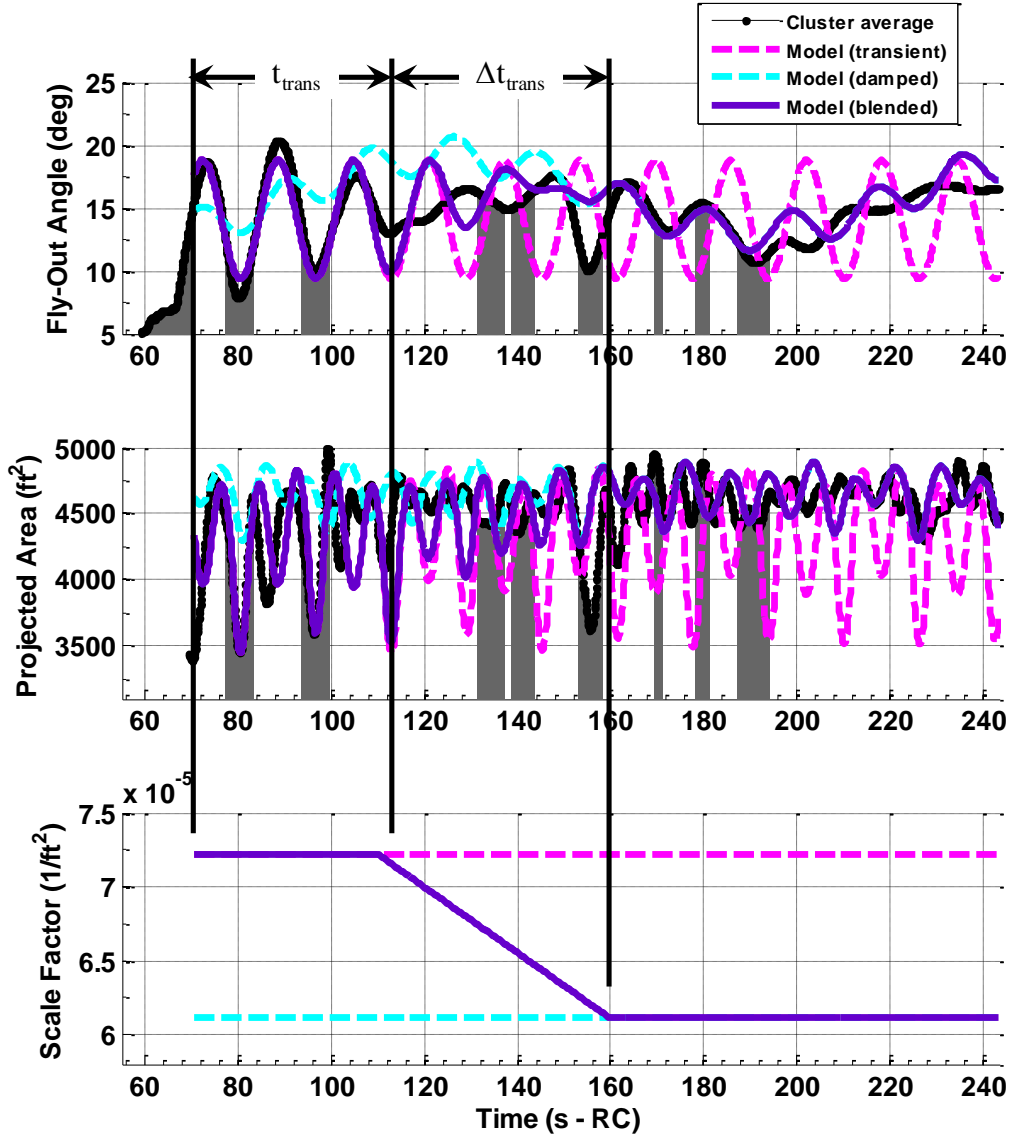American Institute of Aeronautics and Astronautics

Figure 19. **Transient epoch model (magenta) and damped epoch model (cyan) are blended to the final model (purple).**

Once final blended time-varying models of the Main cluster fly-out angle and projected area are generated, these can be converted to the total cluster projected area, S_{pc}. Because the model is assumed to be symmetric, the cluster projected area is a function of the number of parachutes in the cluster, N_c, as shown in Eq. (10).

$$S_{pc}(t) = N_c \cdot S_p(t) \cdot \cos \theta(t) \tag{10}$$

The total cluster projected area is then multiplied by the time-varying scale factor to compute the time-varying drag coefficient according to Eq. (11). The modeled time-varying drag coefficient is compared to the three-Main test data in Fig. 20. Some features present in the test data cannot be captured without adding more complexity to the model (asymmetry, gust response, etc.). However, the model has similar variation as flight test drag, so it should be representative.
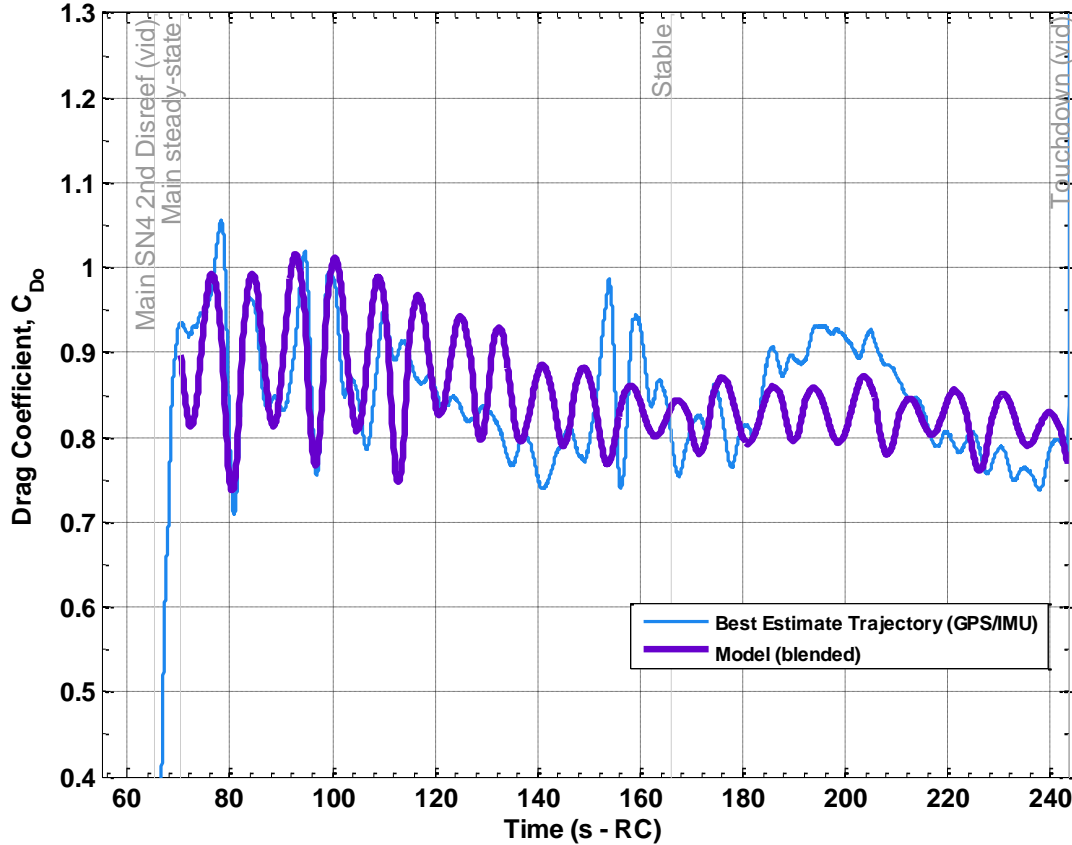
$$C_{Do}(t) = S_{pc}(t) \cdot SF(t) \tag{11}$$

18

American Institute of Aeronautics and Astronautics

Figure 20. **Final time-varying drag coefficient model (purple) compared to CDT-2-3 test data (light blue).**

As with other parameters, the drag coefficient scale factor is dispersed based on the limits from flight test reconstructions. Due to the empirical nature of the model, extrapolation may result in non-realistic simulations. The dispersion tables for two-Main and three-Main cases are documented in the Model Memo.

V. Conclusion

Periodic signal analysis of flight test data has allowed CPAS to develop a time-varying model of steady-state vertical drag coefficient suitable for Monte Carlo simulations. First, the fly-out angles are modeled as the sum of sinusoids with dispersed parameters. Next, individual projected areas are also modeled as sinusoids, with the primary period as half the primary fly-out angle period. The effects of collisions are modeled as sudden losses of projected area. The fly-out angle and projected area models can be combined to generate cluster projected area, which is directly proportional to drag coefficient. This allows for simulating the time-varying nature of drag coefficient and ultimately rate of descent. The time-varying rate of descent model will improve the fidelity of Orion simulations of roll control and splashdown impacts.

Acknowledgments

References

[1] Machín, R. A., Stewart, C. E., Evans, C. T., and McMichael, J. H., "Human Rating the Orion Parachute System," *21st AIAA Aerodynamic Decelerator Systems Technology Conference and Seminar*, Dublin, Ireland, May 2011, AIAA paper 2011-2502.
[2] Morris, A. L., Bledsoe, K. J., Fraire, U., *et al.*, "Summary of CPAS Gen II Testing Analysis Results," *21st AIAA Aerodynamic Decelerator Systems Technology Conference and Seminar*, Dublin, Ireland, May 2011, AIAA paper 2011-2585.

19
American Institute of Aeronautics and Astronautics

[3] Ray, E. and Morris, A. L., "Measurement of CPAS Main Parachute Rate of Descent," *21st AIAA Aerodynamic Decelerator Systems Technology Conference and Seminar*, Dublin, Ireland, May 2011, AIAA paper 2011-2545.

[4] Ray, E., Bretz, D. R., and Morris, A. L., "Photogrammetric Analysis of CPAS Main Parachutes," *21st AIAA Aerodynamic Decelerator Systems Technology Conference and Seminar*, Dublin, Ireland, May 2011, AIAA paper 2011-2538.

[5] Ray, E. and Bretz, D. R., "Improved CPAS Photogrammetric Capabilities for Engineering Development Unit (EDU) Testing," *22nd AIAA Aerodynamic Decelerator Systems Technology Conference*, Daytona Beach, Florida, March 2013, AIAA paper 2013-1258.

American Institute of Aeronautics and Astronautics